Electric to Mechanical Energy Conversion of Linear Ultra-Fast Electro-Mechanical Actuators Based on Stroke Requirements

Ara Bissal, Jesper Magnusson, and Göran Engdahl
Department of Electromagnetic Engineering, Royal Institute of Technology (KTH), 100 44 Stockholm, Sweden

***Abstract*—The operational efficiency of ultra fast actuators used as drives in high voltage direct current breakers are at best 5 %. To boost their efficiency, the design of the energizing circuit is crucial. A multi-physics finite element method (FEM) model coupled with a SPICE circuit model that is able to predict the performance of the actuator with an accuracy of at least 95 % has been developed and verified experimentally. Several variants of prototypes and models have been simulated, built, and tested. It was shown that one of the main problems leading to low efficiencies is the stroke of the drive. However, there is a possibility to increase the efficiency of the electric to mechanical energy conversion process of the studied Thomson (TC) and double sided coils (DSC) to a maximum of 54 % and 88 % respectively if their stroke is minimized. This can be done at the expense of increasing the complexity and the cost of the contact system by designing a switch with several series connected contacts that is encapsulated in a medium with a high dielectric strength. Another proposed solution is to design a current pulse with a rise time that is considerably shorter than the mechanical response time of the system. Parametric variations of capacitances and charging voltages show that the TC and the DSC can achieve efficiencies up to 15 % and 23 % respectively. Regardless of the chosen method, the DSC has a superior efficiency compared to a TC.**

Keywords*—*Capacitance, contacts, electric fields, eddy currents, finite element methods, HVDC circuit breakers, magnetic fields, thermal factors

I. Introduction

THE continuously increasing demand for the generation of bulk power from remote renewable green sources such as solar cells located in deserts or off-shore wind power has rekindled interest in multi-terminal high voltage direct current (HVDC) networks. Recent research is focused on developing power components for HVDC transmission systems such as modular multilevel converters [1]. Although HVDC networks have numerous benefits compared to high voltage alternating current (HVAC), as lower losses, asynchronous interconnections, lower environmental impact, lower investment costs, and added controllability, their adoption relies entirely on the availability of HVDC circuit breakers [2], [3]. Unlike traditional AC systems, HVDC systems have a low impedance and lack a natural current zero crossing. Fault currents increase quickly in magnitude and are harder to manage unless they are interrupted immediately, i.e. within a few milliseconds [4].

Since mechanical breakers are less costly and have lower operating losses compared to semiconductors, this has attracted a lot of research in investigating methods based on ultra-fast electromagnetic drives for separating the current carrying contacts abruptly especially for superconducting fault current limiters [5]. For example, in [6], a Thomson drive is used in a hybrid DC circuit breaker consisting of a mechanical switch, two parallel connected power IGCTs, diodes, and a metal-oxide varistor for dissipating the magnetic energy stored in the grid inductance. In [7], a detailed description showing the vacuum interrupter, the moving contacts, and the bellows of a high speed circuit breaker is given. This circuit breaker has an opening time of 1 ms and a breaking time of around 20 ms. Furthermore, in [8], a rotational drive is implemented with a breaking time of some hundreds of microseconds. Although this drive mechanism can achieve velocities up to 50 m/s, it suffers from an efficiency of less than 5 %. Many other applications for the use of such repulsive forces can be found in [9].

The energy efficiency of these drives is defined by the ratio of the total output kinetic energy and the total input electric energy. Generators or motors can convert electric energy into mechanical energy with efficiencies as high as 99 %. In contrast, state of the art linear ultra-fast actuators based on the Thomson coil (TC) principle have an efficiency of at best 5 %. Although some work has been done on TC actuators such as in [10], [11], [12], and [13]; not much has been done to transduce the electric to kinetic energy with high efficiency using an experimentally validated multi-physics simulation finite element method (FEM) model. The importance of taking into account thermal and mechanical features in addition to electromagnetic features has been shown in [14]. The focus of this paper is on the energizing source that is suitable for each of the studied actuators while taking into consideration the stroke requirements.

II. Description of the HVDC breaker

A DC breaker consists of conducting electrodes, an insulating medium, a control unit, and an ultra-fast drive. When a fault current emerges, the control unit is triggered so that its drive can actuate the contacts promptly. The main purpose of such a DC breaker is to primarily interrupt the fault current, and secondly, to withstand the voltage across its contacts. The voltage withstand level of the breaker depends on several factors some of which are, the insulating medium, the contact separation, the voltage level, humidity, and temperature. However, if required, this stroke can be decreased either by placing

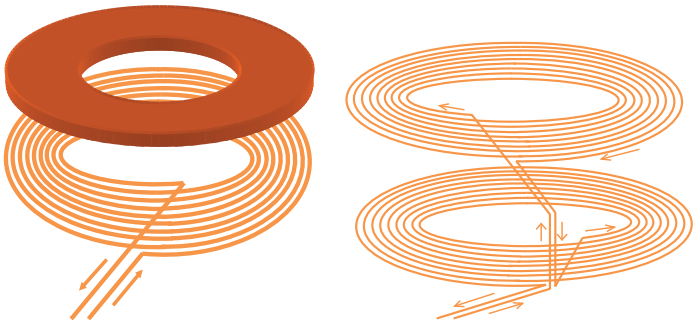

(a) TC (b) DSC

Fig. 1. Sketches of the drives.

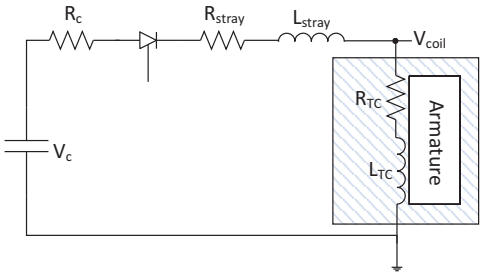

Fig. 2. A diagram showing a circuit model of the capacitor bank and connecting leads of a TC coupled with the FEM model of the TC (shaded) shown in Fig. 1.

the contacts in a medium with a higher dielectric strength such as sulfur hexafluoride (SF6), or by using a number of contacts connected in series by conducting bars to share the total system voltage.

The drive typically used to actuate electrical contacts of ultra-fast breakers is based on the Thomson coil concept. The TC consists of a multi turn flat spiral coil with an electrically conductive material on top, also known as the armature (see Fig. 1a). This armature is attached to a shaft or a push/pull rod whose main purpose is to actuate the electrical contacts and interrupt a fault current. A capacitor bank is discharged to generate large currents that in turn induce currents in the armature due to a varying magnetic field.

A similar candidate that is capable of generating large forces with a slightly higher efficiency than that of a TC without relying on a time varying magnetic field to generate eddy currents in the armature is the double sided coil (DSC) [15]. The current in the armature is injected deliberately by the use of another secondary flat spiral coil that is wound with opposite opposite direction and is series connected with the first coil using a flexible contact as shown in Fig. 1 (b).

III. Modeling

The modeling of the actuator is divided into two parts, a circuit model, and a FEM model implemented in COMSOL Multiphysics. The electrical source consisting of the capacitors, thyristor, and the cable leads connected to a TC or a DSC as shown in Fig. 2 are modeled as a circuit representation while the TC or DSC actuators that are comprised of a primary coil and a mobile armature as shown in Fig. 1 are modeled using a FEM model. These two models are then coupled together and solved simultaneously.

Fig. 2 shows the schematic of the entire system. Once the capacitor bank is charged up to a voltage ($\mathrm{V_C}$), the thyristor is triggered to discharge a current pulse through a TC or a DSC. The bank consists of a combination of several capacitors can be lumped together and modeled as a series RLC network. Since the inductance of the capacitor is in the order of nano Henries, it is significantly smaller than the inductance of the coil and is thereby neglected. As a result, the modeling of the capacitor can be reduced to a capacitance in series with its resistance denoted by $\mathrm{R_C}$. As for the thyristor and cable leads, they are assumed to be frequency independent and are modeled as a lumped impedance comprised of a resistance in series with an inductance denoted by $\mathrm{R_{stray}}$ and $\mathrm{L_{stray}}$ respectively.

The geometry of the actuator is simplified and drawn in a two dimensional axis-symmetric coordinate system to reduce computation time. The coil is modeled as a number of adjacent and insulated rectangles representing its turns. The width and depth of each rectangle corresponds to the cross section of the copper conductor used to wound the coil. The same principle applies for the armature. The magnetic equation is represented by Eq.1, where σ_e is the electrical conductivity, $\mathbf{A}$ is the magnetic vector potential, μ is the magnetic permeability, and $\mathbf{v}$ is the velocity.

$$\sigma_\mathrm{e}\frac{\partial \mathbf{A}}{\partial t} + \frac{1}{\mu}\nabla \times (\nabla \times \mathbf{A}) - \sigma_\mathrm{e}\mathbf{v} \times (\nabla \times \mathbf{A}) = 0 \qquad (1)$$

Electrical machines that conduct large currents may heat up considerably if the conductor cross sections and the cooling system are not dimensioned properly. Similarly, in this case, the resistive losses expressed in Eq. 2 act as a heat source denoted by Q. The temperature increase in the conducting domains is characterized by a heat source and a conductive and a convective term as shown in Eq. 3. The conductive term that is proportional to the thermal conductivity k and the temperature (T) gradient represents the heat flow within the material whereas the convective term, that is proportional to the density of the material (ρ), the heat capacity (C_p), the temperature gradient, and the velocity of the armature, is used to translate the temperature domains within the armature as it is moving away since the model is solved with respect to a stationary reference frame.

Due to small skin depths caused by skin and proximity effects, large temperature differences may occur causing hot spots that deteriorate the electrical conductivity of the material. This is represented by Eq. 4 where σ_{e0} is the electrical conductivity at a reference temperature T_0, and α is the

temperature coefficient.

$$Q = \frac{\mathrm{J}^2}{\sigma_\mathrm{e}} \tag{2}$$

$$\rho C_p(\frac{\partial T}{\partial t} + \mathbf{v}\cdot\nabla T) = \nabla\cdot(k\nabla T) + Q \tag{3}$$

$$\sigma_\mathrm{e} = \sigma_{\mathrm{e}0}[1+\alpha(T-T_0)]^{-1} \tag{4}$$

Currents in the presence of a perpendicular magnetic field result in repulsive electromagnetic forces known as Lorentz forces (**F**) and are described by Eq. 5. If the armature is assumed to be infinitely stiff, then according to Newton's law, its velocity can be computed as shown in Eq. 6 where m is the total mass of both the armature and the copper contacts to be actuated. This velocity can be integrated with respect to time in order to compute the displacement of the armature as shown in Eq. 7. The computed displacement is used to implement a moving mesh based on the Arbitrary Lagrangian-Euler method since the induced forces are highly dependent on the proximity of the armature. The mesh is progressively stretched until a specified stretching factor is violated. Subsequently, the geometry is re-meshed and the cycle is repeated. Finally, the efficiency of the armature (η) is computed as the ratio of the output mechanical energy to the input electrical energy as shown in Eq. 8. v is the end velocity of the armature, C is the net capacitance of the capacitor bank, and V_c is the voltage level that the capacitor bank is charged to.

$$\mathbf{F} = \mathbf{J}\times\mathbf{B} \tag{5}$$

$$\iiint \mathbf{F}\, r\mathrm{d}r\mathrm{d}\theta\mathrm{d}z = m\frac{d\mathbf{v}}{dt} \tag{6}$$

$$\mathbf{x} = \int \mathbf{v}\mathrm{d}t \tag{7}$$

$$\eta = \frac{mv^2}{CV_c^2} \tag{8}$$

IV. Model Verification

The experimental setup consists of a multi-turn flat spiral coil that is embedded in a bakelite housing filled with epoxy. The bakelite is screwed down to a steel plate and the entire structure is clamped down with several steel bars to a massive two ton table to avoid vibrations and keep it firmly in place. The thyristor and a high speed camera that can film with 100000 fps are triggered together. Subsequently, the captured images are calibrated and motion tracking is used to compute the velocity of the armature and compare it with the simulations.

To ensure that the model can accurately predict the behavior of the armature with different configurations, many tests have been done for different variants. The capacitance, armature material and shape, coil shape, load, and charging voltage were varied and tested. Afterwards, these measured velocities were compared with the simulation results. Fig. 3 shows simulations compared with measurements upon the discharge of a 33 mF capacitor bank into a 10 turn flat spiral coil for two armatures, one made of aluminum, and the other made of copper. Subsequently, the voltage was increased from 50 V to 100 V and the simulation and experimental results of the two different armatures are compared once again in Fig. 4. The results clearly show that the simulation model can predict the performance of these ultra-fast drives with an accuracy of 95 %.

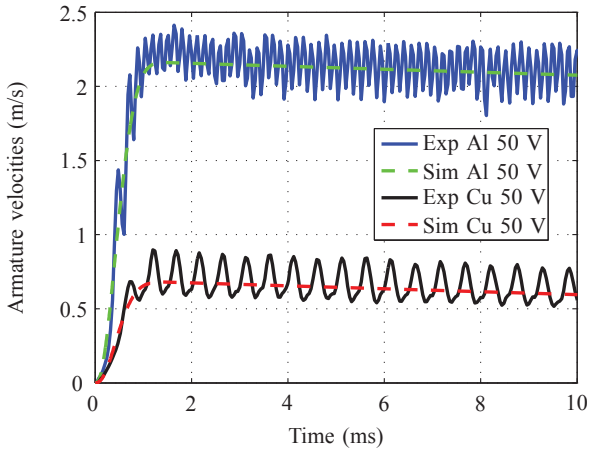

Fig. 3. Simulations compared with experimentally measured armature velocities made of copper and aluminum upon the discharge of a capacitor bank with a capacitance of 33 mF charged up to 50 V.

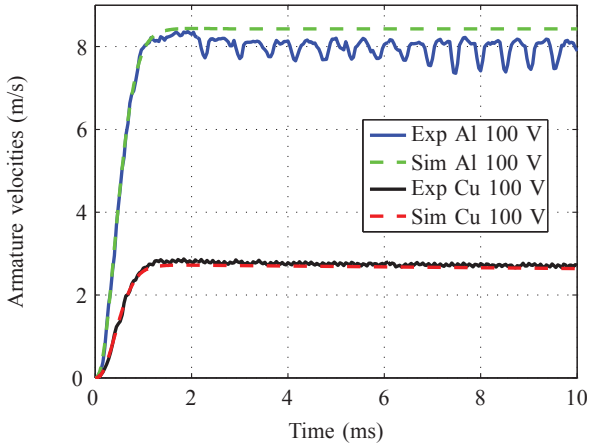

Fig. 4. Simulations compared with experimentally measured armature velocities made of copper and aluminum upon the discharge of a capacitor bank with a capacitance of 33 mF charged up to 100 V.

V. The Challenge of an Ultra-Fast Linear Actuator

Unlike rotating machines, ultra-fast linear actuators have a variable air gap that increases in size as the contacts separate. The final size of the air gap is equal to the required stroke to satisfy the insulation requirement. As such, these actuators suffer from poor efficiencies. Large air gaps result in lower induced currents and lower magnetic field levels. Consequently, the generated repulsive forces decrease significantly

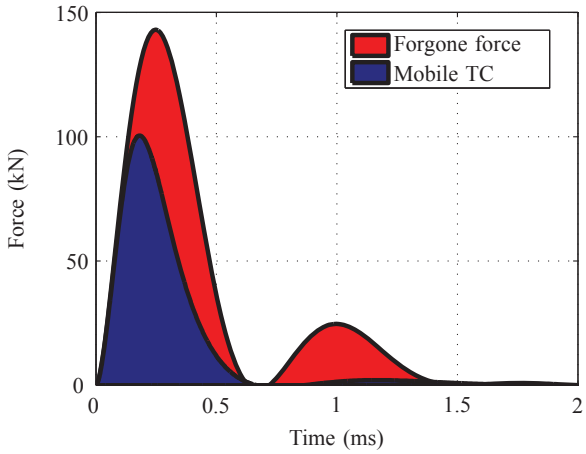

Fig. 5. The force impulse of a mobile TC along with its forgone force due to its stroke. The area shaded in blue is the force impulse of a mobile TC upon the discharge of a 10 mF capacitor bank whereas the area under the curve shaded in red is the forgone force due to the increased air gap with contact separation. In essence, if the armature of the TC is clamped, then the total generated force impulse is given by the sum of the areas under both curves (i.e. the sum of the areas shaded in blue and in red).

with increasing strokes. Fig. 5 demonstrates the forgone force due to a variable air gap upon the discharge of a 10 mF capacitor bank. The forgone force is defined as the computed force upon the discharge of a capacitor bank in an identical system but with a clamped armature. As can be seen, the time integral of the forgone force is quite substantial.

VI. A SUGGESTED DESIGN APPROACH

The efficiency of these actuators can be increased if their stroke is minimized. The system can be designed in such a way to have as many contacts as possible and to use a medium with a high dielectric strength. This increases the complexity and cost of the contact system and enables the drive to operate with much higher efficiencies. However, increasing the complexity of the contact system is not always desirable. Another method for decreasing this forgone force is to dimension a current pulse with a rise time that is considerably smaller than the response time of the mechanical system especially for large stroke applications. In other words, the variables influencing the rise time of the current pulse such as the capacitance will be dimensioned in such a way as to induce the repulsive forces at low air gaps, i.e. prior to any considerable mechanical movement.

The methodology to verify this concept was to use the developed multi-physics simulation model that has been verified with different capacitances, armature materials, voltage levels, and coil sizes. The geometry of the actuator was kept constant in this particular case. Moreover, the load was fixed to 1 kg; a good representative of the contact system. In order to study the influence of the main frequency component of the current pulse on the efficiency of the system, the electrical energy is maintained constant while varying both the charging voltage and the capacitance. If the capacitance is decreased, then frequency of the current pulse increases, leading to smaller skin depths. This is taken into account by reducing the mesh size to a fraction of the skin depth to maintain high accuracy. Furthermore, the time step is also reduced to ensure convergence. The variation of the skin depth can be easily accounted for in the FEM model especially since there are no nonlinearities in the coil and the armature material. In some electrical machines, both the stator and the rotor are made of punched or welded stacks of laminated steel. Due to manufacturing imperfections and the welding process, the material is not homogeneous and can have different properties in different areas. If the frequency content is changed, then the same models may not be able to predict the performance of the machine. When currents are induced with different skin depths, this change is highly dependent on the manufacturing grade and as such, it may be nonlinear and hard to predict. As for the case of the ultra-fast actuators proposed in this paper, the armature of a TC for instance is made of one thick piece of homogeneous copper and is independent of the manufacturing process. Since the material is isotropic, homogenous, and free from manufacturing flaws, the change in skin depth can be easily captured by the model. The same applies to a DSC where the major difficulty lies in designing a flexible contact that can survive several thousands of operations.

VII. ASSESSMENT OF THE APPROACH BY DEVICE SIMULATIONS

The effect on the current by varying the capacitance from 10 µF to 100 mF while maintaining the electrical energy constant is shown in Fig. 6 and Fig. 7. Fig. 6 shows high current densities after 8 µs due to inrush currents and proximity effect. On the other hand, the use of a larger capacitance leads to a rather homogenized current distribution as shown in Fig. 7. The current distributes in such a way as to counteract the change of the magnetic field created by the primary coil due to the injected current. This current distribution is dependent on the time derivative of the current pulse. The larger the time derivative of the current pulse, the more are the oppositely oriented currents in the coil and armature concentrated in the vicinity of each other resulting in smaller skin depths. The current peak due to the discharge of a 10 µF capacitor is larger than that of a 100 mF since inductance decreases with increasing frequencies. However, the primary coil conductor is only partially used rendering its middle and bottom parts almost entirely unused. Therefore, although the effective system inductance is rather small when using a 10 µF capacitor compared to that of a 100 mF, it has a larger effective resistance.

A. TC behaviour and performance

Table I shows the hypothetical armature velocity for a 1 kg load of a clamped TC for different capacitances (C) and charging voltages (Vc). The generated forces from a system with a clamped armature together with the load as used before are used to compute the hypothetical velocity. Although 2640 J of electric energy is used for all cases, the efficiency (η) of the drive is severely influenced based on the partitioning of

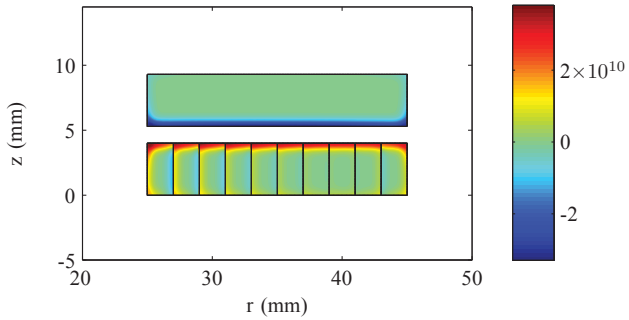

Fig. 6. Current density in (A/m^2) at 8 µs shown in the cross sections of the coil and armature, just before the first current peak, for the first energizing source of a mobile TC shown in Table I.

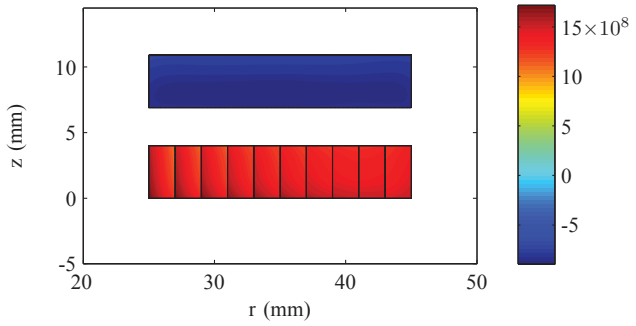

Fig. 7. Current density in (A/m^2) at 500 µs shown in the cross sections of the coil and armature, just before the first current peak, for the last energizing source of a mobile TC shown in Table I.

this energy into capacitance and charging voltage. The drive efficiency can vary from 3.5 % for a 10 µF capacitor up to 53.7 % for a 10 mF capacitor bank. In this case, increasing the capacitance further up to 100 mF causes the efficiency to drop to 26.3 %. This shows that a TC is highly sensitive to the chosen capacitance and charging voltage. For a particular geometry, load, and material, there exists an optimum capacitance and charging voltage.

Reducing the capacitance of the drive circuit and increasing the charging voltage of the energizing source results in a faster electric impulse. At low capacitances, the armature is subjected to higher peak forces and accelerations. The main advantage of using such a configuration system is when a swift contact separation is required. However, this configuration can lead to excessively high impulsive forces that might deform the metallic contacts, bellows, or other fragile components integrated in the system. This can reduce the total number of operations and the lifetime of the switchgear. Although the peak force is increased by utilizing smaller capacitances, the efficiency of the drive is severely deteriorated due to the increased losses from the proximity effect. Large inrush currents concentrate in a thin layer at the top and bottom sides of the primary coil and the armature respectively. This results in a skin depth that is much smaller than the thickness of the

TABLE I. THE EFFICIENCY OF A CLAMPED TC (TC_c), A MOBILE TC (TC_m), A CLAMPED DSC (DSC_c), AND A MOBILE (DSC_m) FOR DIFFERENT ENERGIZING SOURCE CONFIGURATIONS

Energizing source			η (%)			
E (J)	C	V_c	TC_c	TC_m	DSC_c	DSC_m
2640	10 µF	22.978 kV	3.5	2.6	3.9	3.2
2640	100 µF	7.266 kV	11.8	8.1	13.5	9.5
2640	1 mF	2.298 kV	33.1	14.5	40.1	19.1
2640	10 mF	726.64 V	53.7	14.7	75.7	23.2
2640	33 mF	400 V	46.4	10.2	84.5	19.9
2640	100 mF	229.78 V	26.3	5.2	87.7	13.8

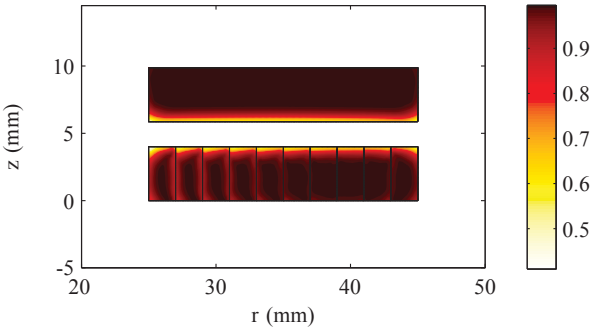

Fig. 8. Electrical conductivity in per unit at 88 µs shown in the cross sections of the coil and armature for the first energizing source shown in Table I.

conductor rendering the rest of the material cross section futile. Consequently, the resistivity of the drive increases decreasing the system efficiency. Moreover, these high current densities cause hot spots that deteriorate the electrical conductivity of the material as shown in Fig. 8. The conductivity in some parts may drop to less than half the initial value although other parts further away from the hot spots remain completely untouched.

A natural way to solve the problems associated with proximity effect is to increase the capacitance and decrease the charging voltage. This reduces the time derivative of the current pulse. A current pulse with a larger rise time results in less losses since the current distributes more evenly in the cross section of the conductor. The current tends to homogenize with increasing capacitances causing the system inductance to increase. Consequently, the temperature rises more or less equally in the material. Due to the absence of large temperature differences, no hot spots occur and the conductivity of the material is left unscathed. Although the generated peak forces decrease, the performance of the drive will still increase since the time integral of the force impulse will be larger. However, this does not hold if the capacitance is infinitely increased since, for a TC, a time varying magnetic flux density is necessary to induce currents in the armature and generate repulsive forces.

There exists an optimum capacitance which the TC should be energized with. Choosing a too small capacitance results in high losses and choosing a relatively large capacitance does not induce enough eddy currents in the armature. An axially oriented time varying magnetic flux density is required to induce oppositely oriented currents in the armature. The product of these induced currents in the armature, together with

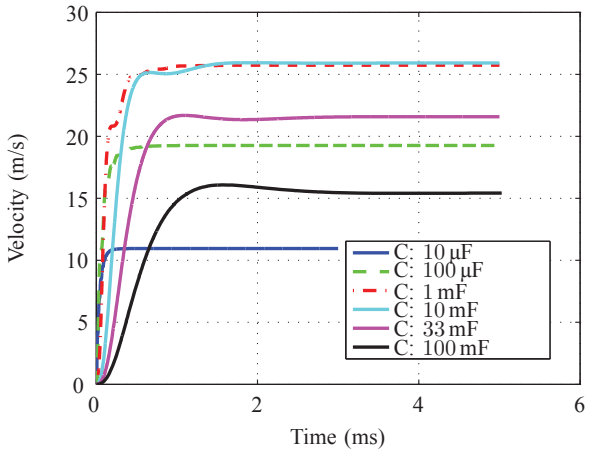

Fig. 9. The velocity profile of a mobile TC drive shown for the six different energizing source cases shown in Table I.

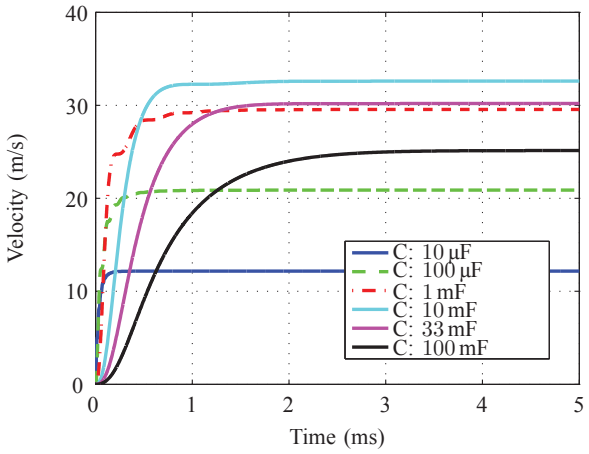

Fig. 10. The velocity profile of a mobile DSC drive shown for the six different energizing source cases shown in Table I.

the confined radial component of the magnetic flux density, generate these required ultra-fast repulsive forces.

When the movement of the armature is taken into consideration, the steady state velocity decreases (Fig. 9) and overall efficiency of the system, regardless of the chosen capacitance, drops significantly. Table I shows that the efficiency of the drive ranges from 2.6 % to a maximum of 14.7 %. This is primarily because the magnetic fields decay with increasing distance from the source and secondly, the induced currents in the armature also decrease in magnitude since they are dependent on the axial component of the field. Therefore, the resultant force that is proportional to the azimuthal currents and the radial field decreases in magnitude with increasing separation.

Although the efficiency of the TC drops for all capacitances when displacement is incorporated, its sensitivity is highly dependent on the chosen capacitance. The drop in efficiency becomes more significant with increasing capacitances. For example, the efficiency of a 100 mF capacitor dropped by 80.2 % while that of a 10 µF capacitor dropped by 25.7 %. This implies that the electrical resonance of the system has to be dimensioned to induce all required forces efficiently, i.e. prior to the movement of the armature. If the capacitance is too high, then as the armature propagates away, the forces are generated at increasing air gaps. This reduces the efficiency of the drive. On the other hand, if the electrical resonance frequency is much higher than the mechanical response, then the generated impulse is unnecessarily fast, causing high losses due to proximity effect. Therefore, for a mobile armature loaded with 1 kg, the best alternative is a capacitance of 1 mF since although it attains almost the same steady state velocity compared to a 10 mF capacitor bank; it has a shorter rise time. Therefore, the armature will arrive its destination in less time.

B. DSC behaviour and performance

Table I shows the velocity profiles for the same capacitances and charging voltages for a clamped DSC. As can be seen, the efficiency of the drive increases with increasing capacitances. Compared to the maximum attained efficiency of 53.7 % for a clamped TC, a clamped DSC can attain efficiencies up to 87.7 %. Unlike a clamped TC, for a clamped DSC, the partitioning of electrical energy into capacitance and charging voltage is relatively easy to justify. The current that flows in the primary coil of a DSC also flows through its secondary mirror coil (also known as armature) but in the opposite direction. Therefore, a time varying magnetic field is not needed to induce currents in the armature. Instead, even when excited continuously with a continuous constant current, a DSC is able to generate massive repulsive forces since an azimuthally oriented current in the presence of a radial field will generate axially directed repulsive forces.

However, steady state speed is only one of the requirements for electric contact separation. Another critical factor in HVDC current interruption is acceleration. Therefore, although increasing capacitance does increase the efficiency of a clamped DSC, it does so at the expense of reduced accelerations and longer rise times.

Although for a clamped DSC, the steady state velocity is maximized by increasing capacitance, for the same reason as discussed for a mobile TC, the resonance frequency of the electrical circuit of a mobile DSC has to be higher than the mechanical response of the system. Therefore, as can be seen in Fig. 10, the efficiency of a mobile DSC loaded mechanically with 1 kg is largest when a 10 mF capacitor is used. Moreover, this shows that the DSC clearly has a superior efficiency compared to a TC.

VIII. Conclusion

Ultra-fast drives such as TCs have been used as mechanisms to generate large enough impulsive forces to be able to interrupt a short circuit current in less than 5 ms. However, unlike rotating electric machines, they suffer from efficiencies as low as 5 % mainly due to an increasing air gap. To increase the performance of these drives, it would be best to design a multi-contact system inserted in a medium with a high dielectric

strength so as to minimize the required stroke. This however is not always desirable due to increased complexity, increased cost, space constraints, and decreased reliability. Therefore, if a large stroke is unavoidable, another method of limiting the loss in efficiency of these drives is to design a current pulse in such a way as to accelerate the armature in only a small fraction of the required stroke as long as it is still in close proximity of the primary coil. After the acceleration phase, the armature can be left to move freely with a constant velocity until it covers the full stroke. By designing a current pulse with a rise time that is much smaller than the mechanical response of the actuator, all repulsive forces will be induced at small air gaps resulting in a higher efficiency. However, a very fast current pulse will lead to excessive losses due to eddy currents. Therefore, this method has a trade-off between the rise time of the current pulse and the associated eddy current losses.

A TC needs a time varying current pulse while a DSC does not when the armature is clamped. For this reason, a DSC can be excited with a DC source and hence will always have a superior efficiency when compared to a TC. If there is a demand for applications with relatively large strokes, then even for a DSC, the armature has to be accelerated in only a fraction of the desired stroke to achieve a high efficiency as mentioned before.

For future work, these preliminary findings will be used as a basis to develop a multi-objective optimization model taking into consideration the coil and armature geometry, size, capacitance, charging voltage, required stroke, and reliability.

ACKNOWLEDGEMENT

This work was in part sponsored by EIT/InnoEnergy through the ESPE project and by SweGRIDS, the Swedish Centre for Smart Grids and Energy Storage, www.swegrids.se.

REFERENCES

[1] R. Feldman, M. Tomasini, E. Amankwah, J. Clare, P. Wheeler, D. Trainer, and R. Whitehouse, "A hybrid modular multilevel voltage source converter for HVDC power transmission," *IEEE Trans. Ind. Appl.*, vol. 49, no. 4, pp. 1577–1588, Jul. 2013.

[2] C. Franck, "HVDC circuit breakers: A review identifying future research needs," *IEEE Transactions on Power Delivery*, vol. 26, no. 2, pp. 998–1007, 2011.

[3] M. Bucher and C. Franck, "Contribution of fault current sources in multiterminal HVDC cable networks," *IEEE Trans. Power Del.*, vol. 28, no. 3, pp. 1796–1803, 2013.

[4] J. Hafner and B. Jacobson, "Proactive hybrid HVDC breakers - a key innovation for reliable HVDC grids," Bologna, Italy, Sep. 2011.

[5] S. Lim, H. Ahn, and C. Park, "Study on fault current limiting characteristics of a SFCL using magnetic coupling of two coils with mechanical switch driven by electromagnetic repulsion force," *IEEE Trans. Appl. Supercon.*, vol. Early Access Online, 2013.

[6] J.-M. Meyer and A. Rufer, "A DC hybrid circuit breaker with ultra-fast contact opening and integrated gate-commutated thyristors (IGCTs)," *IEEE Trans. Power Del.*, vol. 21, no. 2, pp. 646 – 651, Apr. 2006.

[7] T. Takeuchi, K. Koyama, and M. Tsukima, "Electromagnetic analysis coupled with motion for high-speed circuit breakers of eddy current repulsion using the tableau approach," *Electrical Engineering in Japan*, vol. 152, no. 4, pp. 8–16, 2005.

[8] W. Holaus and K. Frohlich, "Ultra-fast switches- a new element for medium voltage fault current limiting switchgear," in *IEEE Power Engineering Society Winter Meeting, 2002*, vol. 1, 2002, pp. 299–304.

[9] I. Boldea, *Linear Electric Machines, Drives, and MAGLEVs Handbook*. CRC Press, Feb. 2013.

[10] W. Li, Y.-w. Jeong, and C.-s. Koh, "An adaptive equivalent circuit modeling method for the eddy current-driven electromechanical system," *IEEE Trans. Magn.*, vol. 46, no. 6, pp. 1859–1862, 2010.

[11] W. Li, Z. Y. Ren, Y.-w. Jeong, and C.-s. Koh, "Optimal shape design of a thomson-coil actuator utilizing generalized topology optimization based on equivalent circuit method," *IEEE Trans. Magn.*, vol. 47, no. 5, pp. 1246–1249, 2011.

[12] M.-T. Pham, Z. Ren, W. Li, and C. S. Koh, "Optimal design of a thomson-coil actuator utilizing a mixed-integer-discrete-continuous variables global optimization algorithm," *IEEE Trans. Magn.*, vol. 47, no. 10, pp. 4163–4166, 2011.

[13] D. Lim, D. Woo, I. Kim, D. Shin, J. Ro, T. Jung, and H. Jung, "Characteristic analysis and design of a thomson coil actuator using an analytic method and a numerical method," *IEEE Trans. Magn.*, vol. Early Access Online, 2013.

[14] X. Sun, M. Cheng, S. Zhu, and J. Zhang, "Coupled electromagnetic-thermal-mechanical analysis for accurate prediction of dual-mechanical-port machine performance," *IEEE Trans. Ind. Appl.*, vol. 48, no. 6, pp. 2240–2248, Nov. 2012.

[15] A. Bissal, J. Magnusson, and G. Engdahl, "Comparison of two ultra-fast actuator concepts," *IEEE Transactions on Magnetics*, vol. 48, no. 11, pp. 3315–3318, 2012.

IX. BIOGRAPHIES

Ara Bissal was born in Beirut, Lebanon in 1986 where he graduated with distinction from the American University of Beirut (AUB) with a B.S. degree in electrical and computer engineering. He then received a M.Sc. degree and a Licentiate degree in electric power engineering from the Royal Institute of Technology (KTH) in 2010 and 2013 respectively. He is currently working half time towards his PhD degree at KTH and at the same time working at ABB AB Corporate Research in Sweden. His main research interests include the design, simulation, and prototype construction of ultra-fast electromechanical actuators that can be used in high voltage direct current (HVDC) circuit breakers.

Jesper Magnusson was born in Stockholm, Sweden in 1984. He received the M.Sc. degree in electrical engineering from the Royal Institute of Technology (KTH), Stockholm, Sweden, in 2010, where he is currently working toward the Ph.D. degree in electrical engineering. His main research interests include electrical switch gear, especially hybrid switches that combine mechanical devices and power electronics.

Göran Engdahl (M89-SM04) was born in Uppsala, Sweden, in 1948. He received the M.Sc., and Ph.D. degrees in electricity from Uppsala University, Uppsala, Sweden in 1974, 1981 respectively. In 2001, he is a Professor of Electrotechnical Design in the Department of Electrical Engineering, Royal Institute of Technology. From 1983 to 1996 Engdahl was active as project manager at ABB working with product development regarding electric power components, where several projects were related to applications with new magnetic and magnetostrictive materials.